Gill paracellular permeability and the osmorespiratory compromise during exercise in the hypoxia-tolerant Amazonian oscar (Astronotus ocellatus)

Lisa M. Robertson, Daiani Kochhann, Adalto Bianchini, Victoria Matey, Vera F. Almeida-Val, Adalberto Luis Val & Chris M. Wood

Journal of Comparative Physiology B
Biochemical, Systems, and Environmental Physiology

ISSN 0174-1578
Volume 185
Number 7

J Comp Physiol B (2015) 185:741-754
DOI 10.1007/s00360-015-0918-4

Springer

J Comp Physiol B (2015) 185:741–754
DOI 10.1007/s00360-015-0918-4

ORIGINAL PAPER

Gill paracellular permeability and the osmorespiratory compromise during exercise in the hypoxia-tolerant Amazonian oscar (*Astronotus ocellatus*)

Lisa M. Robertson[1] · Daiani Kochhann[2] · Adalto Bianchini[3] · Victoria Matey[4] · Vera F. Almeida-Val[2] · Adalberto Luis Val[2] · Chris M. Wood[1,5,6]

Received: 15 March 2015 / Revised: 6 June 2015 / Accepted: 10 June 2015 / Published online: 27 June 2015

Abstract In the traditional osmorespiratory compromise, fish increase their effective gill permeability to O_2 during exercise or hypoxia, and in consequence suffer unfavorable ionic and osmotic fluxes. However oscars, which live in the frequently hypoxic ion-poor waters of the Amazon, actually decrease ionic fluxes across the gills during acute hypoxia without changing gill paracellular permeability, and exhibit rapid paving over of the mitochondrial-rich cells (MRCs). But what happens during prolonged exercise? Gill paracellular permeability, ionic fluxes, and gill morphology were examined in juvenile oscars at rest and during aerobic swimming. Initial validation tests with urinary catheterized fish quantified drinking, glomerular filtration, and urinary flow rates, and confirmed that measurements of gill paracellular permeability as [^{3}H]PEG-4000 clearances were the same in efflux and influx directions, but far lower than previously measured in comparably sized trout. Although the oscars achieved a very similar proportional increase (90 %) in oxygen consumption (MO_2) to trout during steady-state swimming at 1.2 body lengths sec^{-1}, there was no increase in gill paracellular permeability, in contrast to trout. However, oscars did exhibit increased unidirectional Na^+ efflux and net K^+ rates during exercise, but no change in drinking rate. There were no changes in MRC numbers or exposure, or other alterations in gill morphology during exercise. A substantial interlamellar cell mass (ILCM) that covered the lamellae to a depth of 30 % was unchanged by 4 h of swimming activity. We conclude that a low branchial paracellular permeability which can be dissociated from changes in O_2 flux, as well as the presence of the ILCM, may be adaptive in limiting ionoregulatory costs for a species endemic to ion-poor, frequently hypoxic waters.

Keywords Polyethylene glycol (PEG-4000) · Mitochondrial-rich cells (MRCs) · Interlamellar cell mass (ILCM) · Trout · Hypoxia · Cichlid · Exercise · Drinking rate · Glomerular filtration rate

Communicated by G. Heldmaier.

✉ Chris M. Wood
woodcm@mcmaster.ca; woodcm@zoology.ubc.ca

Lisa M. Robertson
lisa.mj.robertson@gmail.com

Daiani Kochhann
daia.kochhann@gmail.com

Adalto Bianchini
adaltobianchini@furg.br

Victoria Matey
vmatey@mail.sdsu.edu

Vera F. Almeida-Val
veraval@inpa.gov.br

Adalberto Luis Val
dalval@inpa.gov.br

[1] Department of Biology, McMaster University, Hamilton, ON L8S 4K1, Canada

[2] Laboratory of Ecophysiology and Molecular Evolution, Instituto Nacional de Pesquisas da Amazônia (INPA), Manaus, AM, Brazil

[3] Universidade Federal do Rio Grande (FURG), Rio Grande, RS, Brazil

[4] Department of Biology, San Diego State University, San Diego, CA 92182, USA

[5] Rosenstiel School of Marine and Atmospheric Science, University of Miami, Miami, FL 33149, USA

[6] Department of Zoology, University of British Columbia, 4200 University Boulevard, Vancouver, BC V6T 1Z4, Canada

Introduction

Classically, the osmorespiratory compromise in fish gills is a permeability trade-off between respiratory gas exchange and unfavorable ionic/osmotic fluxes, such that the latter become greater when the need for the former increases (Randall et al. 1972; Nilsson 1986). The trade-off occurs during exercise or environmental hypoxia when the need to improve O_2 uptake occurs. To date, most studies have focused on the osmorespiratory compromise during swimming activity in highly aerobic fish such as salmonids, showing increased ion and water fluxes (Stevens 1972; Wood and Randall 1973a, b, c; Hofmann and Butler 1979; Wood 1988; Gonzalez and McDonald 1992, 1994; Postlethwaite and McDonald 1995). Several studies have demonstrated comparable effects during hypoxia in salmonids (Thomas et al. 1986; Iftikar et al. 2010; Robertson et al. 2015). It is usually assumed that most of these fluxes are occurring via the paracellular pathway, though this has not been directly demonstrated. However, two recent developments have altered our views on the osmorespiratory compromise.

The first is the discovery of a freshwater fish, the Amazonian oscar (*Astronotus ocellatus*), which shows a very different response, a decrease in branchial ion and water fluxes during environmental hypoxia (Wood et al. 2007, 2009; Richards et al. 2007; De Boeck et al. 2013; Robertson et al. 2015). This cichlid lives in ion-poor water and frequently encounters very low O_2 in its natural environment (Val and Almeida-Val 1995), tolerating levels of 5–20 % air saturation for 20–50 h and up to 6 h of complete anoxia (Almeida-Val and Hochachka 1995; Muusze et al. 1998; Almeida-Val et al. 2000). The congeneric *Astronotus crassipinnis*, which is endemic to the same environment, exhibits very similar hypoxia tolerance (Chippari-Gomes et al. 2005). This decreased ion and water permeability occurs despite an increase in ventilation and O_2 transfer factor of the gills, a measure of effective O_2 permeability (Scott et al. 2008), and is associated with a rapid covering over of the mitochondrial-rich cells (MRCs) by pavement cells (PVCs) (Wood et al. 2009; Matey et al. 2011; De Boeck et al. 2013). In contrast, the rainbow trout (*Oncorhynchus mykiss*) undergoes the traditional osmorespiratory compromise during hypoxia exhibiting an exactly opposite morphological response, increased exposure of the MRCs by PVC retraction (Iftikar et al. 2010; Matey et al. 2011). Therefore, this has led to the new suggestion that most of the decreased or increased ion and water fluxes are occurring by a transcellular pathway through the MRCs, rather than by the paracellular pathway (Wood et al. 2009; Iftikar et al. 2010; Matey et al. 2011).

The second is the development of techniques using radiolabeled polyethylene glycol (MW = 4000; [^{3}H]PEG-4000) for measuring gill paracellular permeability during hypoxia (Wood et al. 2009) and exercise (Robertson and Wood 2014), while accounting for possible errors due to drinking rate and glomerular filtration rate (GFR). In the former study on oscars, gill [^{3}H]PEG-4000 permeability remained constant during severe hypoxia, despite decreased ion and water fluxes, supporting the new interpretation of transcellular permeability adjustments (Wood et al. 2009). In contrast, in the latter investigation on trout, gill [^{3}H]PEG-4000 permeability increased in proportion to O_2 consumption during exercise, supporting the traditional interpretation of paracellular pathway changes (Robertson and Wood 2014). However to date, neither species has been evaluated for paracellular permeability changes during the reciprocal circumstance (i.e. hypoxia for trout, or exercise for oscars).

In the present study, our primary objective was to evaluate branchial paracellular permeability during exercise in the oscar, together with O_2 consumption, ionic flux rates (unidirectional and net Na^+ fluxes, net K^+ and ammonia fluxes) and possible morphological changes in the gills. We hypothesized that the oscar, while adapted for hypoxia, would not be adapted for exercise, and therefore would show the same gill permeability responses as the trout during swimming. There appears to be no previous information on the swimming physiology of oscars.

Paracellular permeability measurements are more complicated in swimming animals, as they must be done in the influx direction, and therefore we first needed to perform the same validation exercises for *Astronotus ocellatus* as used by Robertson and Wood (2014) in *Oncorhynchus mykiss*. These addressed potential complications associated with drinking uptake and urinary losses (i.e. GFR) of the [^{3}H]PEG-4000 marker, and possible rectification of gill permeability (i.e. are influx and efflux permeability comparable?). In this regard, the [^{3}H]PEG-4000 efflux study of Wood et al. (2009), performed on much larger adult oscars at rest, had indicated a much lower gill paracellular permeability than later seen in smaller juvenile trout at rest (Robertson and Wood 2014). While this apparently lower paracellular permeability in oscars would seem to be adaptive for an animal living in ion-poor, frequently hypoxic Amazonian waters (Val and Almeida-Val 1995), it could be an artifact of an eightfold difference in body size, a factor which is well known to greatly influence the metabolic and respiratory physiology of the oscar (Almeida-Val et al. 2000; Sloman et al. 2006). Therefore, a second objective of the present study was to confirm the interspecies difference in baseline paracellular permeability, and possibly other parameters such as GFR and drinking rate, using the

juvenile oscars of the present study which were of similar size (~20 g) to the juvenile trout used by Robertson and Wood (2014). Finally, our morphological examination of the gills of these small oscars revealed an unexpected discovery, so we analyzed some archived samples from our earlier study (Wood et al. 2009) to see if the same structure was present in the gills of large adult oscars (~160 g).

Materials and methods

Experimental animals

All procedures were in compliance with Brazilian national animal care regulations and approved by institutional committees at Instituto Nacional de Pesquisas da Amazônia (INPA) and Universidade Federal do Rio Grande (FURG).

Juvenile Amazonian oscars (*Astronotus ocellatus*) (15–25 g, ~12 cm) were obtained from an aquaculture farm, Sítio dos Rodrigues (Km 35, Rod. AM-010, Brazil), and moved to the Laboratory of Ecophysiology and Molecular Evolution at INPA, in Manaus, AM, Brazil, and for some tests were subsequently transferred to the Institute of Biological Sciences at FURG in Rio Grande, RS, Brazil. This was required to meet different Brazilian radioisotope regulations for the use of [^{3}H] versus [^{22}Na] at the two different locations. At INPA, the composition of the holding and experimental water was [Na^+] = 35 μM, [Cl^-] = 36 μM, [Ca^{2+}] = 18 μM, [Mg^{2+}] = 4 μM, [K^+] = 16 μM, pH = 6.5. At FURG, the composition of the holding and experimental water was [Na^+] = 480 μM, [Cl^-] = 550 μM, [Ca^{2+}] = 330 μM, [Mg^{2+}] = 80 μM, [K^+] = 20 μM, pH = 7.0. At both sites, the fish were held for at least 1 week under a 12-h:12-h light:dark photoperiod prior to experimentation at 28 ± 1 °C, fed daily with commercial pellets (Nutripeixe Tr 36, Purina Co, São Paulo, SP) and starved at least 24 h prior to testing.

Branchial permeability tests with [^{3}H]PEG-4000

These experiments were performed at FURG. Methods follow those developed by Robertson and Wood (2014) where greater detail is provided. The only major difference was a shorter post-cannulation recovery period in oscars (16 h) versus trout (40 h), because of difficulty in keeping the urinary catheters patent over longer periods in oscars.

In brief, for the validation efflux and influx experiments performed on oscars at rest in small chambers, the fish were first fitted with internal urinary bladder catheters. For the validation trials, catheterization was performed while the fish were under anesthesia (0.1 g L^{-1} MS-222 at circumneutral pH) as described by Wood and Patrick (1994). Catheters were fashioned from PE10 tubing, with PE60 sleeves (Clay-Adams™, Becton–Dickinson, Franklin Lakes, NJ, USA) attached by veterinary cyanoacrylate glue (Vetbond™, 3 M Corporation, London, ON, Canada) and anchored to the body wall by silk sutures. The fish were then allowed to recover for 16 h in aerated experimental chambers (600 mL) designed to stop the fish turning and thereby tangling their catheters. Urine flow (siphon head = 3 cm H_2O) was monitored throughout to ensure catheter patency.

Efflux experiments partitioned excretion of the paracellular marker between gills and kidney. Immediately following cannulation, the fish were injected via the caudal haemal arch with 1 μCi [^{3}H]PEG-4000 (Sigma–Aldrich, St. Louis, MO, USA) dissolved in 0.1 mL Cortland saline (Wolf 1963) to allow 16 h for internal equilibration throughout the extracellular space. The water was then changed, marking the start of the 8-h experimental period. Urine was collected continuously, and water samples (5 mL) were taken at 2-h intervals for 8 h, at which time the fish was euthanized.

Influx experiments partitioned the uptake of the paracellular marker between gills and gut, and additionally assessed how much was lost to the urine over the experimental period. After cannulation, fish were similarly placed in 600 mL water for 16 h, then the water was changed and [^{3}H]PEG-4000 (1 μCi) added. Water samples (5 mL) were taken 15 min after dosage to allow for thorough mixing via aeration, marking the start of the 8-h experimental period. This period was short enough to avoid rectal excretion of any ingested [^{3}H]PEG-4000 (Wilson et al. 1996). Urine was again collected continuously, and water samples were taken at 2-h intervals until the fish was euthanized at 8 h.

The results of the above validation trials indicated that it was not necessary to catheterize the fish used in the swimming and parallel control experiments. Therefore, non-catheterized oscars were transferred to 3.2-L (32 × 6 cm) Blazka respirometers and left to settle. Preliminary experiments demonstrated that O_2 consumption (MO_2) declined to stable levels after 2 h and thereafter was stable through 8 h. Furthermore we found that oscars would swim consistently for only about 4 h, and performed best if they had been in the respirometer for a few hours. Therefore, in these experiments, 0–4 h was considered an extended acclimation period during which the fish remained stationary, after which they were left stationary for another 4 h (controls), or else swum at 1.2 body lengths per second (BL/s, experimentals), a speed (~15 cm/s) chosen to match similar previous experiments on trout (Robertson and Wood 2014). [^{3}H]PEG-4000 (1 μCi) was added to the water. Water samples (5 mL) were taken at 2-h intervals, and the fish were euthanized at 8 h. MO_2 was measured in the first, middle, and last hours of the swimming or rest period by periodically closing the respirometry system without aeration

and measuring initial and final partial pressures of oxygen over 10-min intervals with a WTW Oxi325 Oximeter (Weilheim, Germany). Declines in dissolved O_2 concentrations were less than 10 %, and final levels were >70 % saturation. Blanks were performed and found to be negligible. MO_2 was calculated in the usual manner, taking into account fish mass, time, respirometer volume, and O_2 solubility (Boutilier et al. 1984).

At the termination of each experiment, the fish was euthanized by an overdose of MS-222, and a terminal blood sample taken by caudal puncture was immediately centrifuged (5000G, 2 min) for measurement of plasma [^{3}H]PEG-4000 concentration. The body cavity was opened and the gastrointestinal tract was ligated at both ends and carefully removed for determination of [^{3}H]PEG-4000 accumulation by drinking. The whole body (after gut removal) was washed in clean water to remove any superficial marker, then similarly processed for [^{3}H]PEG-4000 accumulation.

Analyses of [^{3}H]PEG-4000

The whole body (everything except the gut) was placed in a 50-mL plastic centrifuge tube with 15 mL of 1 N trace metal grade HNO_3, while the gut, which was more resistant to digestion, was placed into a 15-mL tube to which 5 mL of 2 N nitric acid was added. The sealed tubes were then incubated at 65 °C for 48 h, after which they were centrifuged, and 1 mL of each supernatant was transferred to 20-mL scintillation vials. Ultima Gold scintillation fluid (Perkin-Elmer, Waltham, MA, USA) was added to tissue samples (5 mL fluor: 1 mL nitric acid + tissue), and Perkin-Elmer Opti-phase scintillation fluid was added to water samples (5 mL fluor: 5 mL water). Plasma samples were collected by centrifuging terminal blood samples and adding 100 µL of plasma to 4.9 mL water, while urine samples (variable volume) were made up to 5 mL with water. For both plasma and urine, these 5 mL samples were added to 5 mL Opti-phase fluor. [^{3}H]-PEG-4000 radioactivity (measured in β emissions) was determined using a Packard Tri-carb 2100TR–A210001 scintillation analyser (Perkin-Elmer, Waltham, MA, USA). Plasma, whole body, and gut results were quench-corrected back to a common counting efficiency which was that of the water samples, using the external standard ratio method and quench curves constructed from various amounts of tissue digest or plasma.

[^{3}H]PEG-4000 calculations of branchial paracellular permeability, glomerular filtration rate, and drinking rate

These calculations were performed exactly as reported by Robertson and Wood (2014), using the equations reported there, so they are not repeated here. In brief, in the efflux experiments, urinary [^{3}H]PEG-4000 excretion was the product of urinary flow rate (UFR) times urinary radioactivity, factored by time and fish mass, and branchial [^{3}H]PEG-4000 excretion was the product of the increase in water radioactivity times chamber volume, factored by time and fish mass. Urinary [^{3}H]PEG-4000 clearance rates (equivalent to glomerular filtration rates, GFR) and gill [^{3}H]PEG-4000 efflux clearance rates (i.e. plasma clearance rates) were then calculated by Eqs. 1 and 2 of Robertson and Wood (2014), respectively, using measured final values for plasma radioactivity, and estimated initial values from Eq. 3 of that paper. In influx experiments, gill [^{3}H]PEG-4000 influx clearance rates (i.e. water clearance rates) were calculated from the appearance of radioactivity in the whole body of the fish, with the gut excised (Eq. 4 of Robertson and Wood 2014). Estimates based on the radioactivity of digests of the whole carcass versus those based on measured plasma radioactivity and an assumed ECFV of 193 mL kg^{-1} (see Robertson and Wood 2014) did not differ significantly, and therefore mean values of the two approaches have been reported. Gill efflux clearance rates (plasma clearance) and gill influx clearance rates (water clearance) provide independent estimates of gill paracellular permeability in the two directions. The drinking rate was estimated from the total accumulation of [^{3}H]PEG-radioactivity measured in the excised gastrointestinal tract (Eq. 5 of that paper). To allow direct comparison with data from similarly sized rainbow trout, all rate functions (MO_2, gill clearance rates, GFR, UFR, drinking rates) were scaled to a 20 g fish prior to averaging using a standard mass scaling coefficient to the power of 0.79 from Clarke and Johnson (1999), as outlined in Eq. 6 of Robertson and Wood (2014). This power coefficient is appropriate for oscars of this size (Sloman et al. 2006), though as outlined in the Discussion, a lower value may describe a larger size range in this species (Almeida-Val et al. 1999). These scaled data have also been converted to the more familiar per kilogram basis.

Swimming tests with measurements of ionic flux rates and gill morphology

These experiments were performed at INPA. In swimming and parallel control experiments, non-catheterized oscars were transferred to the same 3.2-L Blazka swimming respirometers as used for the [^{3}H]PEG-4000 trials, and allowed to settle with aeration for 30 min. ^{22}Na (1 µCi; (manufactured by New England Nuclear-Dupont, Boston, MA, USA, and supplied by REM, Sao Paulo, Brazil) was added to the water. After a 15-min mixing period, an initial water sample (10 mL) was taken, and subsequent samples were taken every 2 h until experiment termination at 6 h. In these experiments, 0–2 h was considered an extended acclimation period during which the fish remained stationary,

and fluxes were measured over the 2–6 h period during which fish either continued to remain stationary (controls) or were swum at 1.2 BL/s (experimentals). A 2-h rather than 4-h acclimation period at rest was used in these experiments for logistic convenience, based on the preliminary tests performed in the [^{3}H]PEG-4000 trials (see above), as stable resting MO_2 was reached by 2 h. Water samples were analyzed for ^{22}Na radioactivity, Na^+, K^+, and total ammonia concentrations. A parallel series of experiments with an identical protocol (but without the presence of ^{22}Na) was used for the gill morphology series.

Water ion analyses

Water samples were analyzed for ^{22}Na radioactivity by scintillation counting on a Beckman LS6500 counter (Beckman Coulter, Fullerton, CA, USA), using Ultima Gold scintillation fluid (Perkin-Elmer, Waltham, MA, USA; 5 mL fluor: 5 mL water). Tests showed that quenching was constant so correction was unnecessary. Na^+ and K^+ concentrations were measured via atomic absorption spectrophotometry on an AAnalyst 800 (Perkin-Elmer, Singapore). Water total ammonia concentrations were measured colorimetrically by the salicylate hypochlorite assay (Verdouw et al. 1978).

Ion flux calculations

Na^+ influx (JNa in) was calculated as outlined by Wood (1992) based on ^{22}Na disappearance from water as:

$$\text{JNa in} = \frac{\Delta\text{cpm} \times V}{\text{Average SA} \times M \times \Delta t} \quad (1)$$

where V is the volume of the respirometer (mL), M is the weight of the fish (g), and Δt is the duration of the flux period (4 h). Average specific activity (SA) was determined by averaging initial and final specific activities, the mean ratio of ^{22}Na cpm concentration to total water Na^+ concentration over that time period.

Net Na^+ flux (JNa net) was calculated from the change in the total concentration of Na^+ in the water:

$$\text{JNa net} = \frac{\Delta\text{Na} \times V}{W \times \Delta t} \quad (2)$$

and Na^+ efflux (JNa out) was calculated by difference as:

$$\text{JNa out} = \text{JNa net} - \text{JNa in} \quad (3)$$

Net fluxes for K and total ammonia were calculated by analogy to Eq. 2.

Gill morphology and morphometry

Gills of a total of 16 fish, 8 control (resting) and 8 experimental (swimming for 4 h) were examined by scanning electron microscopy (SEM) and light microscopy (LM). The second gill arches of these fish were dissected out, quickly rinsed, immediately fixed in cold Karnovsky's fixative (Karnovsky 1965) and transported to San Diego State University (SDSU), California, USA. At SDSU, the middle section of each gill arch was cut into 2 equal pieces, each bearing 8–12 filaments in both anterior and posterior rows for SEM and LM studies. These were then rinsed in phosphate buffer saline (PBS), post-fixed in 1 % osmium tetroxide for 1 h, and then dehydrated in ascending concentrations of ethanol from 30 to 100 %. Samples that were used for SEM study were critical-point dried, mounted on the stubs, sputter-coated with platinum, and examined with a Quanta-450 scanning electron microscope (FEI) (Hillboro, OR, USA) at the accelerating voltage of 5–10 kV. The other half of the gill arch was used for LM, and was dehydrated in ethanol, cleared in xylene, and then embedded in paraffin wax. Thick serial paraffin sections at 4–5 mm were cut on a microtome (Microm HM-355, Rhenen, Netherlands), mounted on glass slides, de-waxed in xylene, rehydrated in a descending ethanol series to distilled water, and stained with hematoxylin and eosin. Slides were examined in an Eclipse E200 microscope (Nikon, Melville, NY, USA).

After initial qualitative evaluation of the 8 samples from each treatment group, the 6 best preserved samples of each group were selected for more detailed morphometric examination. The data were based upon 30 measurements per each characteristic (5 randomly selected lamellae in six fish and 5 randomly selected filaments in six fish). Both SEM- and LM-data were used to estimate two characteristics, i.e. the volume of the interlamellar cell mass (ILCM) and the surface area of protruding lamellae. The following parameters were measured to estimate changes in the protruding lamella (PL) surface area and interlamellar cell mass (ILCM) volume: (1) protruding lamella height (determined by LM); (2) protruding lamella thickness (determined by LM); (3) basal length of protruding lamella (determined by SEM); (4) ILCM height (determined by LM); and (5) distance between two adjacent lamellae (determined by LM). The surface areas of protruding lamellae were calculated using parameters 1–3, and the volume of the ILCM was calculated using parameters 3–5 according to Sollid et al. (2003).

To calculate the surface area for the protruding lamellae an estimation of the area based on half of an ellipse was made as follows:

$$a = pL \quad (4)$$

where a is the respiratory surface area of the lamellae, L is the basal length of the protruding lamellae, and p is the ellipse perimeter formula divided by 2:

$$p = \frac{2\pi\sqrt{(1/2)(r^2 + h^2)}}{2} \quad (5)$$

and

$$r = t/2 \quad (6)$$

where h is the height of the protruding lamellae and t is the thickness of the lamellae. The volume (V) of the interlamellar cell mass (ILCM) was calculated as a rectangular solid:

$$V = dhL \quad (7)$$

where d is the distance between two adjacent lamellae, h is the height of ILCM and L is the basal length of the protruding lamella.

SEM data were also used to estimate the number of openings of MRCs per mm^2 and for calculation of the surface area of apical crypts of individual MRC's. The number of MRC openings was counted on five randomly selected areas for six fish in control (rest) and six fish in experimental treatment (swimming) on the trailing edge of the filament behind the respiratory lamellae on SEM microphotographs (2000× magnification). The surface area of individual apical crypts of MRC's was calculated on SEM microphotographs (4500× and 3700× magnifications) of the surface of 5–7 cells for each of six fish examined in control and experimental treatments. The measurements were done on the cells positioned "en face" that made the full cell surface visible.

Archived samples of gills of resting adult oscars (141–180 g; $N = 4$) from the study of Wood et al. (2009) were examined using the same techniques.

Statistics

Data have been expressed as the means ± 1 SEM (N). Student's unpaired two tailed t test ($P < 0.05$) was employed to compare all exercise versus resting measurements, as well as measurements of gill [^{3}H]PEG-4000 permeability in the efflux versus influx directions, and the distribution of [^{3}H]PEG-4000 radioactivity between different compartments, and morphometric differences between small and large oscars, with the Bonferroni correction for multiple comparisons. Percentage data were arc-sin transformed prior to testing.

Results

Data from the efflux and influx validation tests have been tabulated together with comparable data from similarly sized rainbow trout (Robertson and Wood 2014) in Table 1 as one of the key objectives was comparison of the two species (see "Introduction").

[^{3}H]PEG-4000 efflux tests

In these tests on resting oscars, [^{3}H]PEG-4000 had been injected into the vascular system of the fish 16 h before the start of the 8-h test period. UFR was low, only about 50 % of that in trout (Table 1), but a high percentage (91.2 %) of the total [^{3}H]PEG-4000 excretion occurred via the urine, with only 8.8 % effluxing via the gills (Fig. 1a). These values translated to a high GFR, about 2.7-fold greater than in trout, and a low gill plasma clearance rate, only 25 % of that in trout (Table 1).

[^{3}H]PEG-4000 influx tests

These tests on resting oscars measured the partitioning of [^{3}H]PEG-4000 uptake from the water between the

Table 1 Measurements in resting juvenile oscars (*Astronotus ocellatus*) of gill ^{3}[H]PEG-4000 permeability, expressed as clearance rates, in the efflux (gill plasma clearance rate) and influx directions (gill water clearance rate), together with corresponding measurements of glomerular filtration rate (GFR) and urine flow rate (UFR) in the efflux experiments, and drinking rate in the influx experiments

	Oscars ($N = 5$)		Trout[a] ($N = 12$–14)	
	(ml 20 g^{-1} h^{-1})	(ml kg^{-1} h^{-1})	(ml 20 g^{-1} h^{-1})	(ml kg^{-1} h^{-1})
Efflux				
Gill plasma clearance	0.050 ± 0.015*	2.49 ± 0.76*	0.193 ± 0.029	9.60 ± 1.45
GFR	0.572 ± 0.083*	28.60 ± 4.15*	0.210 ± 0.028	10.50 ± 1.40
UFR	0.068 ± 0.015*	3.40 ± 0.61*	0.138 ± 0.018	6.90 ± 0.90
Influx				
Gill water clearance	0.100 ± 0.023*	5.00 ± 1.15*	0.259 ± 0.041	12.95 ± 2.05
Drinking rate	0.009 ± 0.002	0.45 ± 0.10	0.066 ± 0.020	3.32 ± 0.98

The data are compared with corresponding measurements in comparably sized juvenile rainbow trout (*Oncorhynchus mykiss*) using identical techniques (data from Robertson and Wood 2014). Note that the data are presented allometrically scaled for a typical 20-g fish, and also then translated to the more traditional per kg basis (see text for details). Means ± 1 SEM (N)

There were no significant differences ($P > 0.05$) between clearance rates measured in the efflux versus influx direction in either species

* Significant difference ($P < 0.05$) from corresponding trout data

[a] Trout data from Robertson and Wood (2014)

carcass (83.4 %), gut (7.7 %), and loss to urine (8.9 %) over the 8-h period (Fig. 1b). Based on the sum of the carcass and urinary radioactivity, these values translated to a relatively low gill water clearance rate which was only 39 % of the comparable value in trout (Table 1). In oscars, the gill water clearance rate was not significantly different from the gill plasma clearance rate measured in the efflux trials, similar to the situation in trout (Table 1). Therefore in both species, [^{3}H]PEG-4000 permeability is effectively the same in the influx versus efflux directions. Drinking rate was also low in the oscars, only 13 % of the mean trout value, although the latter difference was not significant because of high variability in the trout data (Table 1).

[^{3}H]PEG-4000 tests with swimming fish

Based on the data from the validation trials, it would only be possible to measure gill [^{3}H]PEG-4000 permeability in the efflux direction in swimming oscars if the fish were cannulated, so as to allow correction for the high urinary losses through GFR (Fig. 1a; Table 1). Catheter drag would undoubtedly interfere with exercise performance in these small fish. However, when measured over the same time frame in the influx direction, urinary [^{3}H]PEG-4000 losses were very small relative to branchial uptake of the radiolabel (Fig. 1b). Therefore, using the influx technique, urinary cannulation can be avoided and the influence of drinking uptake can be eliminated by gut excision prior to carcass processing. Thus, the influx approach was used to estimate branchial [^{3}H]PEG-4000 permeability in the swimming trials.

Oscars did not appear to be strong sustained swimmers, and 4 h at 1.2 BL sec seemed to be close to their endurance capacity. This exercise regime caused an approximate doubling of MO_2 (Fig. 2b) but no significant change in the gill water clearance rate of [^{3}H]PEG-4000 (Fig. 2a) which remained close to values measured in the validation trials on resting oscars (Table 1). Thus, exercise did not elevate gill paracellular permeability despite the increase in O_2 flux. Drinking rate also did not change with swimming activity (Fig. 2c).

Ionic flux rates of swimming fish

Continuous swimming for 4 h at 1.2 BL/s resulted in some disturbances in ionoregulatory parameters (Fig. 3). The unidirectional efflux rate of Na^+, and the net loss rate of K^+ both approximately doubled, but corresponding increases in unidirectional Na^+ influx rate and net Na^+ loss rates were not significant. There was no change in ammonia excretion rate.

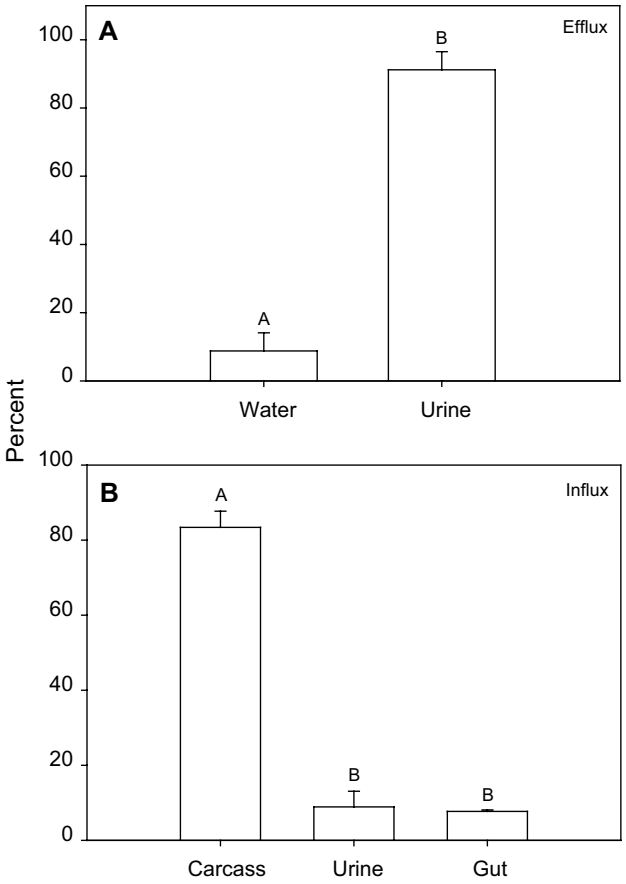

Fig. 1 Relative fate of [^{3}H]PEG-4000 cpm after 8 h in the efflux and influx series on resting juvenile oscars (*Astronotus ocellatus*). **a** Data from the efflux series in which [^{3}H]PEG-4000 was injected into fish fitted with urinary bladder cannulae ($N = 5$). The % of the total [^{3}H]PEG-4000 cpm excreted to the water and in the urine is shown. **b** Data from the influx series in which [^{3}H]PEG-4000 uptake from the water into the carcass, gastrointestinal tract (gut), and urine was monitored in fish fitted with urinary bladder cannulae ($N = 5$). The % of the total [^{3}H]PEG-4000 cpm recovered in each of the three compartments is shown. Means ± 1 SEM. *Bars* not sharing the same letter are significantly different ($P < 0.05$) within each panel

Gill morphology and morphometry of swimming fish

Both qualitative and quantitative analyses showed no detectable differences in general morphology of gills in oscars at rest and those swimming for 4 h at 1.2 BL/s (Figs. 4, 5). In both resting and swimming fish, long filaments supported long and roughly triangular lamellae covered by a thin epithelium (Figs. 4a–d, 5). In both groups, a multilayered interlamellar cell mass (ILCM) covered almost 30 % of the lamellar height (Fig. 5; Table 2). No quantitative differences were found between major parameters of gill filaments and lamellae such as lamellar surface area, height of protruding lamellae and ILCM volume (Table 2). Furthermore, neither the number of MRCs

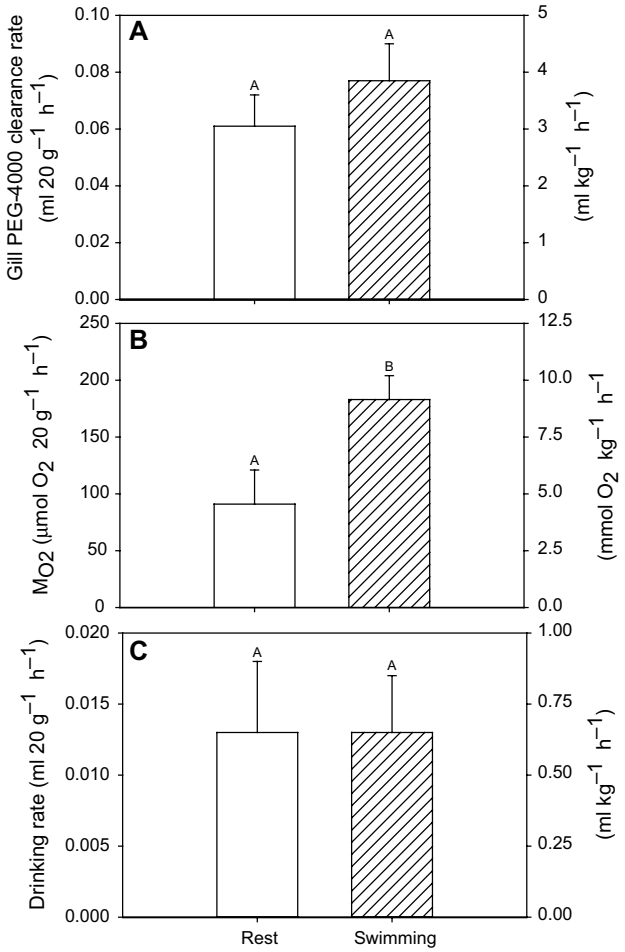

Fig. 2 The influence of 4 h of continuous swimming ($N = 8$) versus rest ($N = 8$) in juvenile oscars (*Astronotus ocellatus*) on: **a** branchial ^{3}[H]PEG-4000 permeabilities, expressed as gill water clearance rates measured in the influx direction; **b** oxygen consumption rates (MO_2); and **c** drinking rates. Mean ± SEM. Note that the data are presented as allometrically scaled for a typical 20-g fish on the left-hand axis, and also translated to the more traditional per kg basis on the right-hand axis (see text for details). Means ± 1 SEM. *Bars* not sharing the *same letter* are significantly different ($P < 0.05$) within each panel

exposed to the water nor the mean surface areas of their apical crypts were altered in swimming fish relative to resting fish (Table 2).

A substantial ILCM was found in these juvenile oscars (Table 2). As parameters of ILCM were not studied in our earlier projects on adult oscars (see "Discussion"), we therefore re-examined archived samples from large adult fish (~160 g) using light microscopy to determine the size of the ILCM, as well as scanning electron microscopy for other characteristics. This exercise confirmed that the ILCM in adult oscars was of comparable relative size to that of young fish, covering approximately 30 % of the lamellar height (Table 2). As expected, most branchial dimensional measurements were significantly larger in the adult oscars (Table 2). However, the mean surface areas of the MRC apical crypts were significantly greater in juveniles, and there was a tendency (non-significant) for a greater density of MRCs on their gill filaments (Table 2). There was also a qualitative difference inasmuch as MRCs were distributed only along the trailing edges of filaments and were never seen on the lamellae in juvenile oscars, whereas they occurred at both locations in adult oscars.

Discussion

Overview

The validation tests with juvenile oscars confirmed that measurements of gill paracellular permeability as ^{3}[H]PEG-4000 clearances were the same in efflux and influx directions at rest, as previously demonstrated in juvenile rainbow trout. Therefore, paracellular permeability could be measured in the influx direction in swimming trials. The validation tests also revealed some marked differences from comparably sized trout in absolute branchial ^{3}[H]PEG-4000 permeability (far lower in oscars), as well as in GFR (much higher in oscars) and UFR (lower in oscars). These measurements confirmed that gill paracellular permeability was really much lower in oscars than in trout, though differences in fish size in a comparison based on earlier data had exaggerated the extent of the difference. Our hypothesis that oscars, being adapted for hypoxia tolerance rather than exercise, would show the same gill permeability responses as the trout during swimming was only partially confirmed. Although the oscars exhibited a very similar proportional increase in MO_2 during steady-state swimming, there was no increase in gill paracellular permeability, in contrast to trout. There was also no change in MRC numbers or exposure, or other alterations in gill morphology during exercise. On the other hand, oscars did exhibit increased ion flux rates during swimming as in trout. The morphological studies also revealed the presence of a substantial ILCM in both juvenile and adult oscars, which had been overlooked in previous studies on adult members of the species. The presence of the ILCM was unchanged by 4 h of swimming activity.

Validation tests in resting oscars and comparison with trout

^{3}[H]PEG-4000 clearance rates from the plasma (i.e. efflux measurements) and from the water (i.e. influx measurements) did not differ significantly, similar to earlier findings on trout (Robertson and Wood 2014). Therefore, ^{3}[H]PEG-4000 moves with equal ease in either direction across the branchial epithelium, and gill paracellular permeability

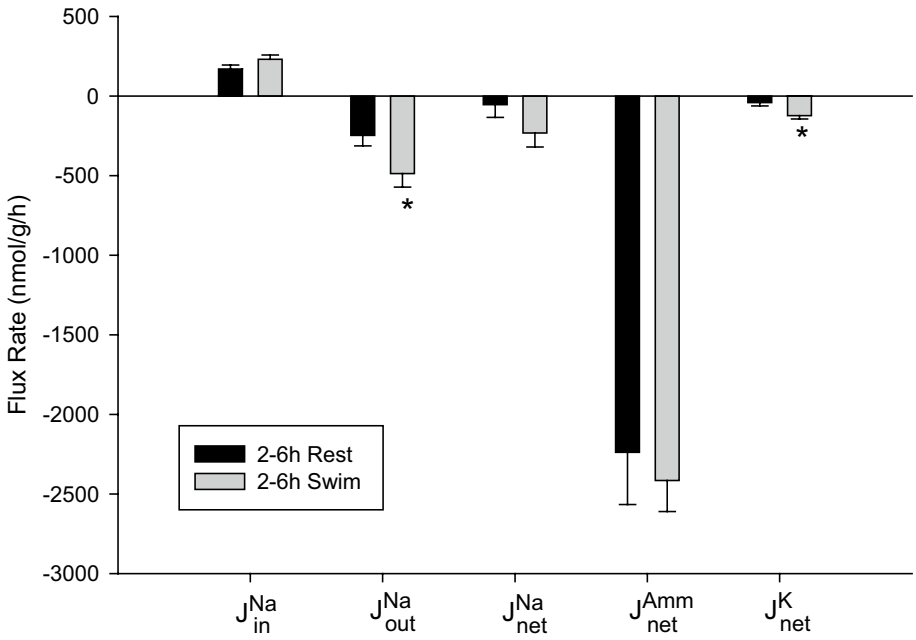

Fig. 3 Unidirectional Na^+ flux rates (influx and efflux) and net Na^+, K^+ and total ammonia flux rates in juvenile oscars (*Astronotus ocellatus*) at rest or during 4 h of continuous swimming at 1.2 BL/s. *Positive values* represent uptake from the water into the fish, *negative values* represent loss from the fish to the water. Means ± 1 SEM ($N = 12$–16). *Asterisks* indicate significant differences ($P < 0.05$) between swimming and resting values

is not rectified. However, there were some marked differences from trout. Firstly, the fate of injected [^{3}H]PEG-4000 radioactivity was very different between the two species, with over 90 % of the total [^{3}H]PEG-4000 excretion occurring via the urine, and less than 10 % via the gills in juvenile oscars (Fig. 1a), whereas in trout, approximately 50 % occurred by each route (Robertson and Wood 2014). The present findings on juvenile oscars are in agreement with earlier work on adult oscars showing that 95 % of injected [^{3}H]PEG-4000 was cleared through the urine, and only 5 % through the gills (Wood et al. 2009). This interspecies difference reflects two influences: much lower gill paracellular permeability and a much higher GFR in oscars.

Using the average of three mean values (the influx and efflux estimates of the validation trials in Table 1, and the resting measurements in the swimming respirometers in Fig. 2), branchial [^{3}H]PEG-4000 clearance rate was about 0.070 mL 20 g^{-1} h^{-1} (3.50 mL kg^{-1} h^{-1}) in juvenile oscars at rest. This may be compared with an average of 0.230 mL 20 g^{-1} h^{-1} (11.50 mL kg^{-1} h^{-1}) for the same measurements in juvenile trout of the same size (Robertson and Wood 2014). Thus, gill paracellular permeability at rest is 70 % lower in oscar versus trout of similar size, despite the much higher temperature in oscars (28 °C versus 18 °C). This value for resting juvenile oscars may also be compared with the earlier measurement (only in the efflux direction) for resting adult oscars of Wood et al. (2009), also at 28 °C. Using a standard mass coefficient to the power of 0.79 (Clarke and Johnson 1999), as confirmed by Sloman et al. (2006) for small oscars, to scale the adult oscar data (160 g) to the juvenile size (20 g), the branchial [^{3}H]PEG-4000 clearance rate would be only 0.62 mL kg^{-1} h^{-1}. However, over a size range of 40–400 g, Almeida-Val et al. (1999) reported a much lower mass scaling power for MO_2 of only 0.52 in *Astronotus ocellatus*. Using this value, the branchial [^{3}H]PEG-4000 clearance rate would be 1.09 mL kg^{-1} h^{-1} in 20-g fish, still much lower than in juvenile oscars. Regardless of which power is used, it is evident that while branchial paracellular permeability is very low in juvenile oscars relative to trout, it is even lower in adult oscars, in accord with the mass-related differences in resting MO_2 and hypoxia tolerance in this species (Almeida-Val et al. 1999; Sloman et al. 2006). The presence of the ILCM may contribute to this low gill permeability (see below). Clearly, the low branchial paracellular permeability in the oscar would seem to be adaptive for life in ion-poor Amazonian waters, as would the low drinking rate (Table 2). However, measurements on a range of different species living in a variety of water qualities will be required to confirm the generality of these observations, and/or to look for a phylogenetic signal in the data.

In contrast to gill [^{3}H]PEG-4000 clearance rate, GFR was much higher in oscars than in trout at rest, a 2.7-fold difference (Table 2). The oscar values (28.60 mL kg^{-1} h^{-1} in juveniles) are at the high end of the range of previous determinations in freshwater fish (see summaries in Hickman and Trump 1969; Wood and Patrick 1994), but are in agreement with similarly high values recorded in adult oscars by Wood et al. (2009): 13.92–24.41 mL kg^{-1} h^{-1} depending on which scaling power is used, as discussed earlier. It is remarkable that resting GFR's are so high in oscars, when UFRs are actually lower than in trout

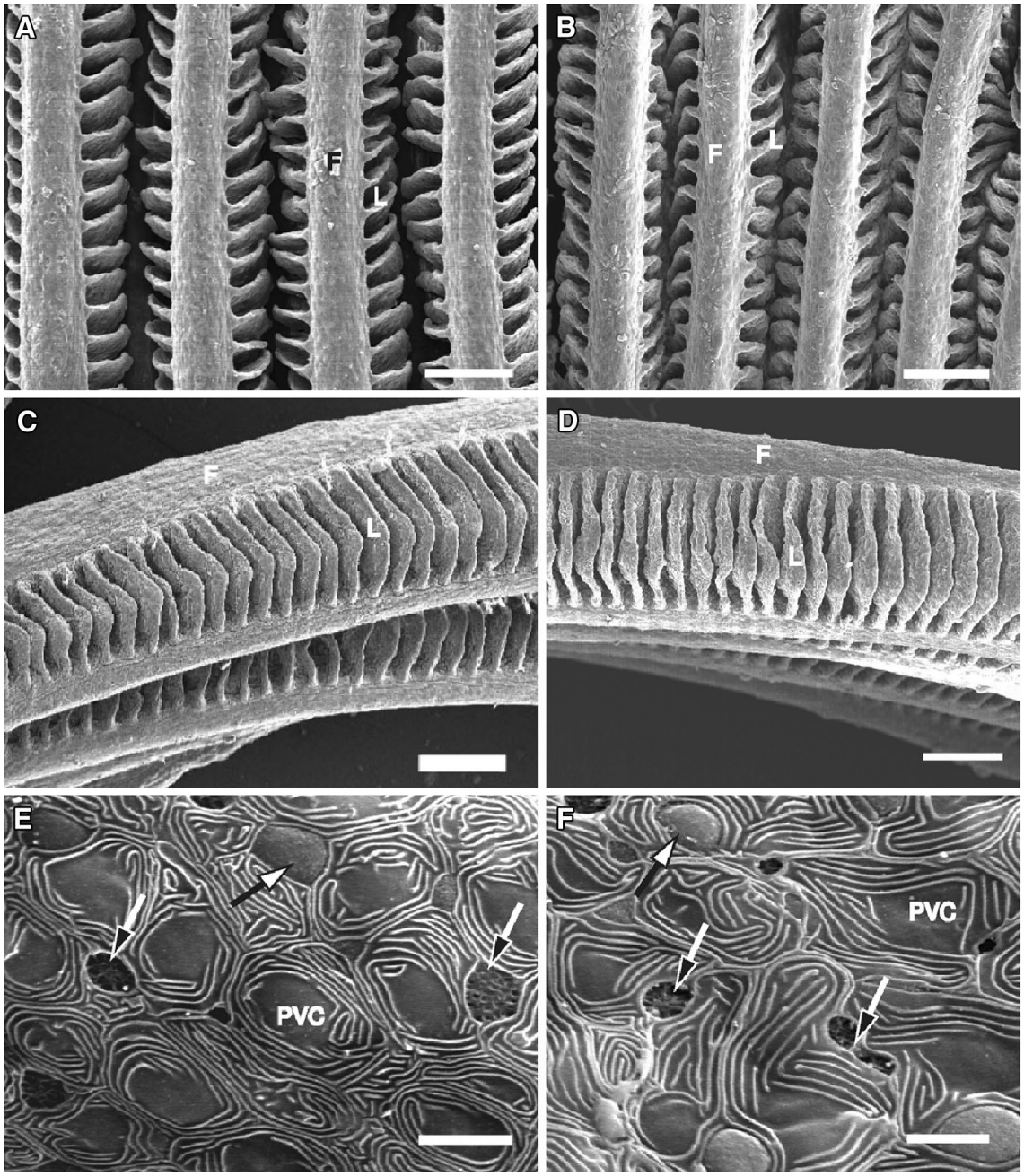

Fig. 4 Representative scanning electron micrographs of gill filaments from juvenile oscars (*Astronotus ocellatus*) at rest (**a**, **c**, **e**; controls) and after 4 h of continuous swimming (**b**, **d**, **e**). **a** *Frontal view* of gill filaments supporting long lamellae. **b** *Frontal view* of gill filaments. No difference between **a** and **b**. **c** *Side view* of gill filament. Note roughly *triangular shape* of lamellae. **d** *Side view* of gill filament. No difference between **c** and **d**. **e** Surface of trailing edge of gill filament. Note relief of pavement cells composed of long microridges, apical crypts of mitochondrial-rich cells with a flat and sieve-like surface, and large openings of mucous cells. **f** Surface of trailing edge of gill filament does not differ from that depicted in **e**. *F* filament, *L* lamella, *PVC* pavement cell. *Black-head arrows* designate mitochondrial-rich cells (MRCs), *white-head arrows* designate mucous cells (MCs). *Scale bars* **a**, **b** 100 μm; **c**, **d** 50 μm; **e**, **f** 5 μm

(Table 2) and many other teleosts (Hickman and Trump 1969; Wood and Patrick 1994). The low UFR must reflect low branchial permeability to water, but the high GFR necessitates high rates of ion and water reabsorption in the kidney, so its adaptive significance is unclear.

Responses to exercise and gill morphology

During steady-state exercise at 1.2 BL/s for 4 h, juvenile oscars increased their MO_2 by 92 % (Fig. 2a), very comparable to the 75 % increase in juvenile trout swimming at

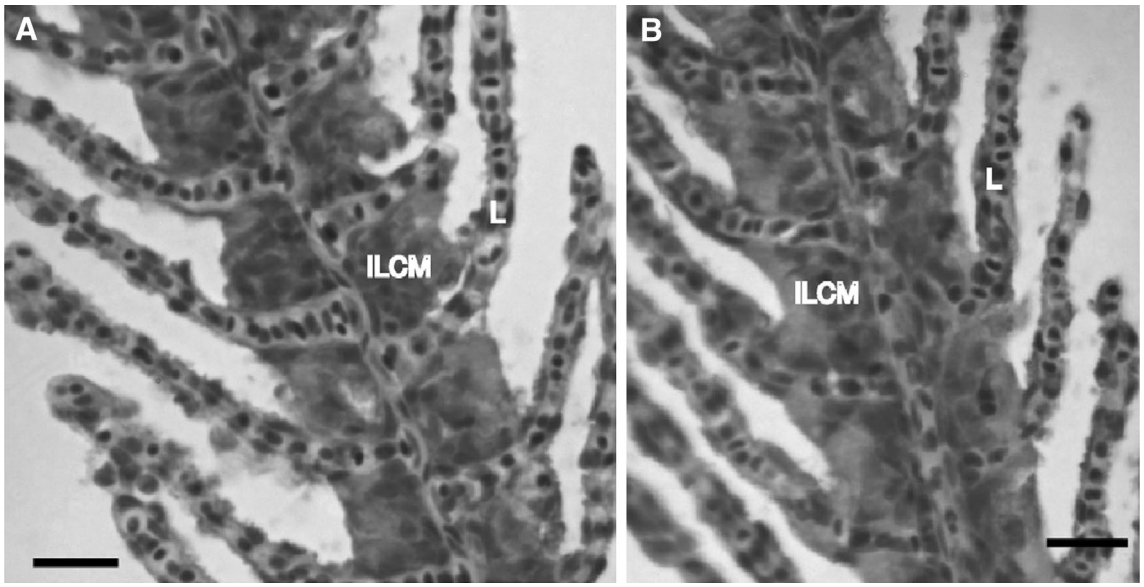

Fig. 5 Representative light micrographs of gill filaments in oscars (*Astronotus ocellatus*) at rest (**a**) and after 4 h of continuous swimming (**b**). **a** Middle part of gill filament. Note multilayered interlamellar cell mass and lamellae covered by thin epithelium. **b** Middle part of gill filament. No difference between **a** and **b**. *F* filament, *ILCM* interlamellar cell mass, *L* lamella. *Scale bars* 20 μm

Table 2 Morphometric characteristics of gills from juvenile oscars (*Astronotus ocellatus*) at rest (control) or after 4 h of swimming at 1.2 BL/s

	Juveniles (~20 g)		Adults (~160 g)
	Resting ($N = 6$)	Swimming ($N = 6$)	Resting ($N = 4$)
Total lamella height (μm)	82.9 ± 1.7	83.0 ± 1.4	123.9 ± 4.6*
Protruding lamellar height (*h*) (μm)	60.0 ± 0.5	60.0 ± 0.7	84.1 ± 4.5*
Percent of lamellar height embedded into filament epithelium (%)	28.2 ± 0.9	28.1 ± 0.7	31.6 ± 1.8
Basal length (*L*) (μm)	78.6 ± 0.5	78.4 ± 0.4	198.1 ± 0.7*
Lamellar thickness (*t*) (μm)	5.9 ± 0.3	5.8 ± 0.7	11.1 ± 0.3*
ILCM height (μm)	23.4 ± 0.3	23.3 ± 0.3	39.1 ± 2.5*
Distance between lamellae (*d*) (μm)	19.8 ± 0.5	19.9 ± 0.8	29.3 ± 1.6*
ILCM volume (*V*) (μm^3)	3.64×10^{4a}	3.64×10^{4a}	22.7×10^{4}*
Individual lamellar surface area (*A*) (μm^2)	10,483[a]	10,457[a]	54,559[a]
No. of MRC apical crypt openings/mm^2 of filament trailing edge	1911 ± 111	1961 ± 116	1691 ± 24
Apical surface area of individual crypt (μm^2)	6.7 ± 0.3	6.2 ± 0.4	5.6 ± 0.3*

Means ± 1 SEM. Data for resting adult oscars are also shown

There were no significant differences ($P > 0.05$) between swimming and resting juvenile oscars

* Significant difference ($P < 0.05$) between resting adult and resting juvenile oscars

[a] Values without SEM were calculated from group means

the same speed in the same respirometers (Robertson and Wood 2014). Note, however, that despite the 10 °C higher temperature, the absolute MO_2 values under both conditions were only about 60 % of those in trout. The resting rates in oscars were very similar to those recorded by Sloman et al. (2006) for juveniles of a similar size. Relative to general predictive relationships of MO_2 versus temperature established for all teleosts (e.g. Clarke and Johnson 1999), the resting rates for oscars are low, while those for trout are high, as might be expected for a tropical, hypoxia-tolerant species versus a temperate, highly aerobic species.

Despite the increase in MO_2, juvenile oscars exhibited no significant increase in gill paracellular permeability during exercise (Fig. 2b), in contrast to juvenile rainbow trout (Robertson and Wood 2014). This measurement was made as the influx [^{3}H]PEG-4000 clearance rate from the

water, so we applied the same small correction for unmeasured GFR losses to both treatment groups (from data in Fig. 1b), using the same calculation procedure as in trout (discussed by Robertson and Wood 2014). If the GFR had increased during exercise by 23 % as reported by Hofmann and Butler (1979) for trout, then there would still have been no significant change in branchial paracellular permeability in the oscars. Therefore, oscars are able to elevate O_2 flux through the branchial epithelium without increasing paracellular permeability. This is in agreement with the responses during acute hypoxia where oscars are able to increase the transfer factor for O_2 across the gills (a measure of branchial O_2 permeability; Scott et al. 2008) without increasing paracellular permeability (Wood et al. 2009). Clearly the two processes can be dissociated in the oscar, a valuable characteristic for a species which inhabits ion-poor, frequently hypoxic waters.

Nevertheless, oscars did exhibit increased unidirectional effluxes of Na^+ and net losses of K^+ during exercise (Fig. 3), in contrast to the decreases in these parameters seen during acute hypoxia (Wood et al. 2007, 2009; De Boeck et al. 2013; Robertson et al. 2015). During hypoxia, these flux reductions were attributed to decreased transcellular permeability associated with a rapid morphological response, a reduction in exposed MRC numbers and mean apical crypt surface areas due to a paving over by PVCs (Wood et al. 2009; Matey et al. 2011; De Boeck et al. 2013). However, during exercise, there was no opposite morphological response in oscar gills (Table 1), so increased ionic fluxes can presumably occur through some other mechanism. Indeed all measured dimensions of the gills remained unchanged after 4 h of exercise in oscars, very different from the substantial and divergent changes seen in a much shorter period during acute hypoxia in oscars versus trout (Matey et al. 2011).

The presence of the ILCM

All fish have "the interlamellar filament epithelium with a high concentration of functionally important cells" (Conte 1969), but the presence of a distinct ILCM in this area was first described in the gills of the crucian carp (a cyprinid) which is undoubtedly the most hypoxia-tolerant of all teleosts (Sollid et al. 2003). Therefore, in hindsight, it is perhaps predictable that it would also be prominent in the oscar, which is also extremely tolerant of hypoxia (see "Introduction"; Almeida-Val and Hochachka 1995; Muusze et al. 1998; Almeida-Val et al. 2000). We were initially surprised by its presence in juvenile oscars, because we had not noted it in our earlier morphological studies on the gills of adult oscars acclimated to the same ion-poor water (Wood et al. 2009; Matey et al. 2011; De Boeck et al. 2013). In those earlier investigations on adult oscars, we had not used light microscopy (LM) which facilitates detection of this structure. However, the current analysis of archived samples from Wood et al. (2009) confirmed that the ILCM was similarly present in adult oscars, and was of comparable relative size to that in juveniles.

To our knowledge, this is only the second report of the presence of the ILCM in a cichlid fish; Johannsson et al. (2014) noted its presence in the Magadi tilapia. However, the report of Chapman et al. (2000) that African cichlids reared in a hypoxic environment had larger lamellae might have reflected regression of the ILCM. Previously, the ILCM has also been found in a variety of cyprinids (e.g. Sollid et al. 2003, 2005; Matey et al. 2008; Perry et al. 2010, 2012; Smith et al. 2012; Dhillon et al. 2013) and cyprinodonts (e.g. Ong et al. 2007; Barnes et al. 2014). The function of the ILCM is generally thought to be minimization of unfavorable ionic and osmotic fluxes under conditions where some restriction of respiratory gas exchange is tolerable (Sollid and Nilsson 2006; Nilsson 2007). For example, in crucian carp and goldfish, it is present at close to 100 % coverage in resting fish at cold temperatures, but is reduced or eliminated when the fish are exercised or acclimated to high temperatures (Sollid et al. 2003, 2005; Sollid and Nilsson 2006; Nilsson 2007; Perry et al. 2010, 2012; Brauner et al. 2011; Smith et al. 2012). Its presence in the oscar at about 30 % lamellar height, even at relatively high temperature (28 °C), and after 4 h of exercise (Table 2; Fig. 5) may be an important factor explaining the low gill paracellular permeability. The ILCM may well be adaptive in reducing ionoregulatory and osmoregulatory costs in this species which lives in an ion-poor environment and which has relatively low metabolic rate (Sloman et al. 2006), high blood O_2 affinity (Robertson et al. 2015), and high hypoxia tolerance (Almeida-Val and Hochachka 1995; Muusze et al. 1998; Almeida-Val et al. 2000). In future studies, it will be of interest to see if the ILCM in the oscar decreases in volume, thereby allowing greater protrusion of the lamellae and increasing the surface area for gas exchange during prolonged hypoxia exposure or exercise, or at very high temperature, or if it proliferates at colder temperatures leaving shorter lamellae and decreasing the surface area of the gills.

Acknowledgments Supported in Manaus, Brazil by FAPEAM and CNPq through the INCT-ADAPTA grant to ALV, and Ciência sem Fronteiras grant to ALV and CMW, in Rio Grande, Brazil by an award from the International Development Research Centre (IDRC) and the Canada Research Chair Program to AB and CMW, and an award from CNPq to AB in the scope of INCT-TA, and in Canada by a Natural Sciences and Engineering Research Council of Canada (NSERC) Discovery grant to CMW. LMR was supported by an Ontario Graduate Scholarship. DK was a recipient of a PhD fellowship from CNPq. CMW was supported by the Canada Research Chairs program, and is the recipient of a fellowship from the Science Without Borders Program (CNPq-Brazil). ALV, VFAV, and AB are recipients of research

fellowships from CNPq, and AB is also supported by the International Research Chair Program of IDRC. We thank two anonymous reviewers for constructive comments.

References

Almeida-Val VMF, Hochachka PW (1995) Air-breathing fishes: metabolic biochemistry of the first diving vertebrates. In: Mommsen TP (ed) Hochachka PW. Environmental and ecological biochemistry, Amsterdam, pp 45–55

Almeida-Val VMF, Paula-Silva MN, Duncan WP, Lopes NP, Val AL, Land SC (1999) Increase of anaerobic potential during growth of an Amazonian cichlid, *Astronotus ocellatus*. Survivorship and LDH regulation after hypoxia exposure. In: Val AL, Almeida-Val VMF (eds) Biology of tropical fishes. INPA, Manaus, pp 437–448

Almeida-Val VMF, Val AL, Duncan WP, Souza FCA, Paula-Silva MN, Land SC (2000) Scaling effects on hypoxia tolerance in the Amazon fish *Astronotus ocellatus* (Perciformes: Cichlidae): contribution of tissue enzyme levels. Comp Biochem Physiol B 125:219–226

Barnes KR, Cozzi RR, Robertson G, Marshall WS (2014) Cold acclimation of NaCl secretion in a eurythermic teleost: mitochondrial function and gill remodeling. Comp Biochem Physiol A 168:50–62

Boutilier RG, Heming TA, Iwama GK (1984) Appendix: physicochemical parameters for use in fish respiratory physiology. In: Hoar WS, Randall DJ (eds) Fish physiology, vol 10. Academic Press, New York, pp 403–430

Brauner CJ, Matey V, Zhang W, Richards JG, Dhillon R, Cao ZD, Fu S-J (2011) Gill remodeling in crucian carp during sustained exercise and the effect on subsequent swimming performance. Physiol Biochem Zool 84:535–542

Chapman LJ, Galis F, Shinn J (2000) Phenotypic plasticity and the possible role of genetic assimilation: hypoxia-induced trade-offs in the morphological traits of an African cichlid. Ecol Lett 3:387–393

Chippari-Gomes AR, Gomes LC, Lopes NP, Val AL, Almeida-Val VM (2005) Metabolic adjustments in two Amazonian cichlids exposed to hypoxia and anoxia. Comp Biochem Physiol B 141:347–355

Clarke AJ, Johnson NM (1999) Scaling of metabolic rate with body mass and temperature in teleost fish. J Anim Ecol 68:893–905

Conte FP (1969) Salt secretion. In: Hoar WS, Randall DJ (eds) Fish physiology, vol 1. Academic Press, New York, pp 241–292

De Boeck G, Wood CM, Iftikar FI, Matey V, Scott GR, Sloman KA, da Silva MDNP, Almeida-Val VMF, Val AL (2013) Interactions between hypoxia tolerance and food deprivation in Amazonian oscars, *Astronotus ocellatus*. J Exp Biol 216:4590–4600

Dhillon RS, Yao L, Matey V, Chen B-J, Zhang AJ, Cao Z-D, Fu S-J, Brauner CJ, Wang YS, Richards JG (2013) Interspecific differences in hypoxia-induced gill remodeling in carp. Physiol Biochem Zool 86:727–739

Gonzalez RJ, McDonald DG (1992) The relationship between oxygen consumption and ion loss in a freshwater fish. J Exp Biol 163:317–332

Gonzalez RJ, McDonald DG (1994) The relationship between oxygen uptake and ion loss in fish from diverse habitats. J Exp Biol 190:95–108

Hickman C, Trump B (1969) Kidney. In: Hoar WS, Randall D (eds) Fish physiology, vol 1. Academic Press, New York, pp 211–212

Hofmann EL, Butler DG (1979) The effect of increased metabolic rate on renal function in the rainbow trout, *Salmo gairdneri*. J Exp Biol 82:11–23

Iftikar F, Matey V, Wood CM (2010) The ionoregulatory responses to hypoxia in the freshwater rainbow trout *Oncorhynchus mykiss*. Physiol Biochem Zool 83:343–355

Johannsson OE, Bergman HL, Wood CM, Laurent P, Kavembe DG, Bianchini A, Maina JN, Chevalier C, Bianchini LF, Papah MB, Ojoo RO (2014) Air breathing in the Lake Magadi tilapia *Alcolapia grahami*, under normoxic and hyperoxic conditions, and the association with sunlight and ROS. J Fish Biol 84:844–863

Karnovsky MJ (1965) A formaldehyde glutaraldehyde fixative of high osmolality for use in electron microscopy. J Cell Biol 27:137–139

Matey V, Richards JG, Wang Y, Wood CM, Rogers J, Davies R, Murray BW, Chen XQ, Du J, Brauner CJ (2008) The effect of hypoxia on gill morphology and ionoregulatory status in the Lake Qinghai scaleless carp, *Gymnocypris przewalskii*. J Exp Biol 211:1063–1074

Matey V, Iftikar FI, De Boeck G, Scott GR, Sloman KA, Almeida-Val VMF, Val AL, Wood CM (2011) Gill morphology and acute hypoxia: responses of mitochondria-rich, pavement, and mucous cells in two species with very different approaches to the osmorespiratory compromise, the Amazonian oscar (*Astronotus ocellatus*) and the rainbow trout. Can J Zool 89:307–324

Muusze B, Marcon J, van den Thillart G, Almeida-Val VMF (1998) Hypoxia tolerance of Amazon fish. Respirometry and energy metabolism of the cichlid *Astronotus ocellatus*. Comp Biochem Physiol A 120:151–156

Nilsson S (1986) Control of gill blood flow. In: Nilsson S, Holmgren S (eds) Fish physiology: recent advances. Croom Helm, London, pp 87–101

Nilsson GE (2007) Gill remodelling in fish—a new fashion or an ancient secret? J Exp Biol 210:2403–2409

Ong KJ, Stevens ED, Wright PA (2007) Gill morphology of the mangrove killifish (*Kryptolebias marmoratus*) is plastic and changes in response to terrestrial air exposure. J Exp Biol 210:1109–1115

Perry SF, Schwaiger T, Kumai Y, Tzaneva V, Braun MH (2010) The consequences of reversible gill remodeling on ammonia excretion in goldfish (*Carassius auratus*). J Exp Biol 213:3656–3665

Perry SF, Fletcher C, Bailey S, Ting J, Bradshaw J, Tzaneva V, Gilmour KM (2012) The interactive effects of exercise and gill remodeling in goldfish (*Carassius auratus*). J Comp Physiol B 182:935–945

Postlethwaite E, McDonald DG (1995) Mechanisms of Na and Cl regulation in freshwater-adapted rainbow trout (*Oncorynchus mykiss*) during exercise and stress. J Exp Biol 198:295–304

Randall DJ, Baumgarten D, Malyusz M (1972) The relationship between gas and ion transfer across the gills of fishes. Comp Biochem Physiol A 41:629–637

Richards JG, Wang YS, Brauner CJ, Gonzalez RJ, Patrick ML, Schulte PM, Choppari-Gomes AR, Almeida-Val VMF, Val AL (2007) Metabolic and ionoregulatory responses of the Amazonian cichlid, *Astronotus ocellatus*, to severe hypoxia. J Comp Physiol B 177:361–374

Robertson LM, Wood CM (2014) Measuring gill paracellular permeability with polyethelene glycol-4000 in freely swimming trout: proof of principle. J Exp Biol 217:1425–1429

Robertson LM, Val AL, Almeida-Val VF, Wood CM (2015) Ionoregulatory aspects of the osmorespiratory compromise during acute environmental hypoxia in 12 tropical and temperate teleosts. Physiol Biochem Zool 88:357–370

Scott GR, Wood CM, Sloman KA, Iftikar FI, De Boeck G, Almeida-Val VMF, Val AL (2008) Respiratory responses to progressive hypoxia in the Amazonian oscar, *Astronotus ocellatus*. Respir Physiol Neurobiol 162:109–116

Sloman KA, Wood CM, Scott GR, Wood S, Kajimura M, Johannsson OE, Almeida-Val VMF, Val AL (2006) Tribute to R. G. Boutilier: the effect of size on the physiological and behavioural

responses of oscar, *Astronotus ocellatus*, to hypoxia. J Exp Biol 209:1197–1205

Smith AA, Zimmer AM, Wood CM (2012) Branchial and extra branchial ammonia excretion in goldfish (*Carassius auratus*) following thermally induced gill remodelling. Comp Biochem Physiol A 162:185–192

Sollid J, Nilsson GE (2006) Plasticity of respiratory structures—adaptive remodelling of fish gills induced by ambient oxygen and temperature. Respir Physiol Neurobiol 154:241–251

Sollid J, De Angelis P, Gundersen K, Nilsson GE (2003) Hypoxia induces adaptive and reversible gross morphological changes in crucian carp gills. J Exp Biol 206:3667–3673

Sollid J, Weber RE, Nilsson GE (2005) Temperature alters the respiratory surface area of Crucian carp *Carassiuscarassius* and goldfish *Carassiusauratus*. J Exp Biol 208:1109–1116

Stevens ED (1972) Changes in body weight caused by handling and exercise in fish. J Fish Res Bd Can 29:202–203

Thomas S, Fievet B, Motais R (1986) Effect of deep hypoxia on acid-base balance in trout: role of ion transfer processes. Am J Physiol 250:R319–R327

Val AL, Almeida-Val VMF (1995) Fishes of the Amazon and their environment. Physiological and biochemical features. Springer, Heidelberg, p 224

Verdouw H, van Echted CJA, Dekkers EMJ (1978) Ammonia determination based on indophenol formation with sodium salicylate. Water Res 12:399–402

Wilson RW, Gilmour KM, Henry RP, Wood CM (1996) Intestinal base excretion in the seawater-adapted rainbow trout: a role in acid-base balance? J Exp Biol 199:2331–2343

Wolf K (1963) Physiological salines for fresh-water teleosts. Prog Fish Cult 25:135–140

Wood CM (1988) Acid-base and ionic exchanges at gills and kidney after exhaustive exercise in the rainbow trout. J Exp Biol 146:461–481

Wood CM (1992) Flux measurements as indices of H^+ and metal effects on freshwater fish. Aquat Toxicol 22:239–264

Wood CM, Patrick ML (1994) Methods for assessing kidney and urinary bladder function in fish. In: Hochachka PW, Mommsen TP (eds) Biochemistry and molecular biology of fishes, vol 3. Elsevier, New York, pp 127–143

Wood CM, Randall DJ (1973a) The influence of swimming activity on sodium balance in the rainbow trout (*Salmo gairdneri*). J Comp Physiol 82:207–233

Wood CM, Randall DJ (1973b) Sodium balance in the rainbow trout (*Salmo gairdneri*) during extended exercise. J Comp Physiol 82:235–256

Wood CM, Randall DJ (1973c) The influence of swimming activity on water balance in the rainbow trout (*Salmo gairdneri*). J Comp Physiol 82:257–276

Wood CM, Kajimura M, Sloman KA, Scott GR, Walsh PJ, Almeida-Val VMF, Val AL (2007) Rapid regulation of Na^+ fluxes and ammonia excretion in response to acute environmental hypoxia in the Amazonian oscar, *Astronotus ocellatus*. Am J Physiol 292:R2048–R2058

Wood CM, Iftikar FI, Scott GR, De Boeck G, Sloman KA, Matey V, Valdez Domingos FX, Duarte RM, Almeida-Val VMF, Val AL (2009) Regulation of gill transcellular permeability and renal function during acute hypoxia in the Amazonian oscar (*Astronotus ocellatus*): new angles to the osmo respiratory compromise. J Exp Biol 212:949–964